

Supporting Information

Structural Interplay in Block Copolymer-Bile Salt Complexes: From Globules to Ribbons

Suelen Gauna Trindade,^{1,2} Guanqun Du,^{1,#} Luciano Galantini,³ Lennart Piculell,¹ Watson Loh,^{2} and Karin Schillén^{1*}*

¹ Division of Physical Chemistry, Department of Chemistry, Lund University, P.O. Box 124, SE-22100 Lund, Sweden.

² Institute of Chemistry, University of Campinas (UNICAMP), P.O. Box 6154, 13083-970, Campinas, São Paulo, Brazil.

³ Department of Chemistry, Sapienza University of Rome, P.O. Box 34-Roma 62, Piazzale A. Moro 5, 00185 Roma, Italy.

Present address: Physical and Chemical Analysis Center at Suzhou Institute for Advanced Research, University of Science and Technology of China, Suzhou 215123, People's Republic of China.

*Corresponding authors: wloh@unicamp.br; karin.schillen@fkem1.lu.se

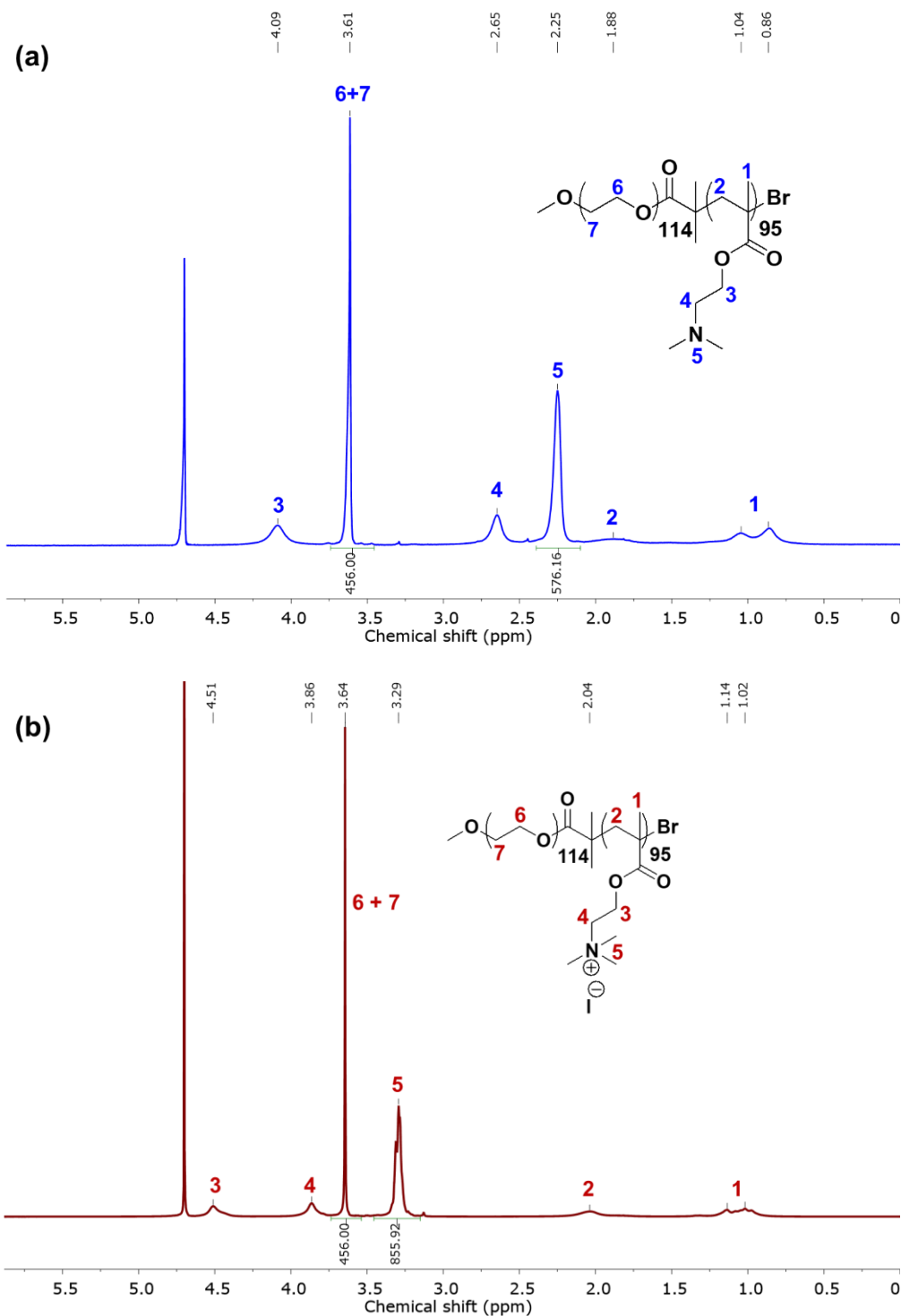


Figure S1. ^1H NMR spectra in D_2O of (a) $\text{PEO}_{114}\text{-}b\text{-PDMAEMA}_{95}$ copolymer before quaternization and of (b) $\text{PEO}_{114}\text{-}b\text{-PTMAEMA}_{95}$ obtained after quaternization. In both spectra, the well-resolved peak of the methylene groups of the PEO block (peak 6+7) at $\delta = 3.64$ ppm was used as internal reference for integration. The integral of the PEO peak was normalized to the total number of methylene protons in the PEO block ($n_{\text{H,tot,PEO}} = n_{\text{H,rep,PEO}} \times N_{\text{PEO}} = 4 \times 114 = 456$ protons). Since the number of PEO protons is unaffected by the quaternization, we may then directly compare the integral of the trimethylammonium signal 5 in (b) with that of the dimethylamino signal 5 in (a). (Note also that the latter peak is completely absent in (b).) The ratio is 1.486, compared to the value of 1.5 for complete quaternization.

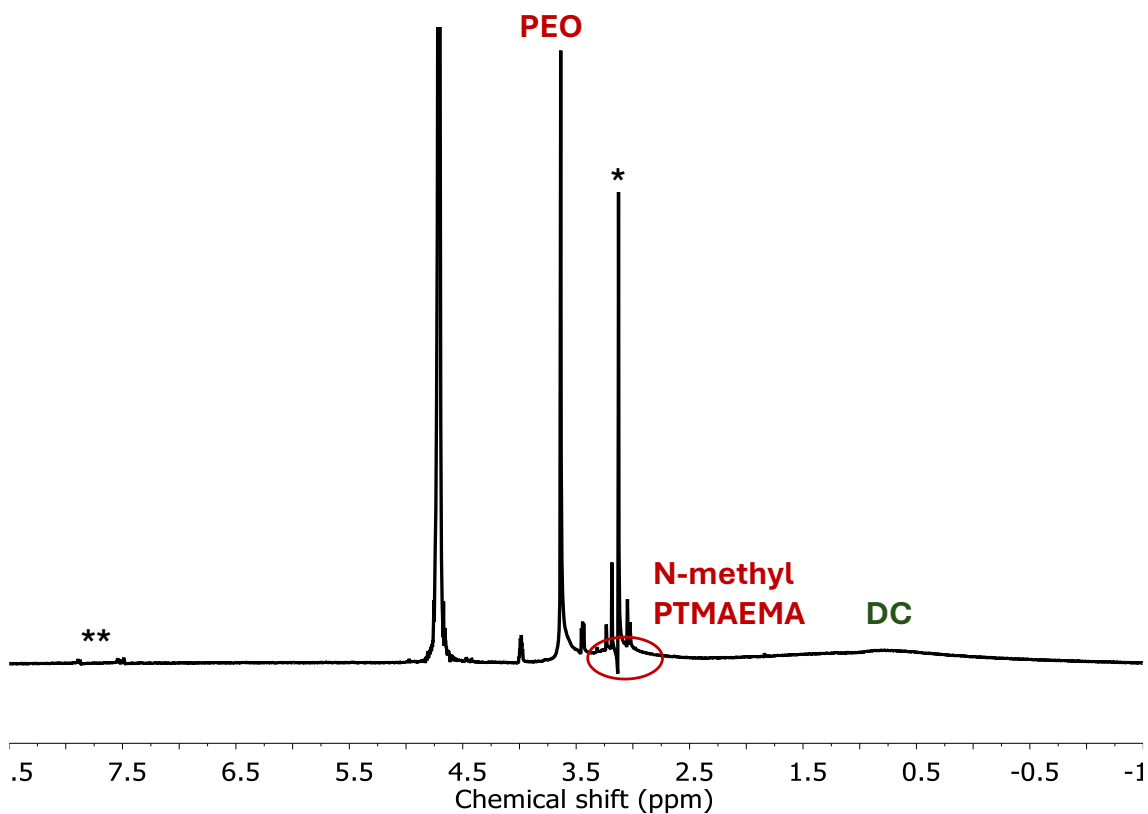


Figure S2. ^1H NMR spectra in D_2O of the PEO DC complex salt sample. Peaks signed by (*) and (**) correspond to trimethylamine and poly(vinyl)methacrylate, respectively, which are subproducts of the Hofmann elimination reaction.

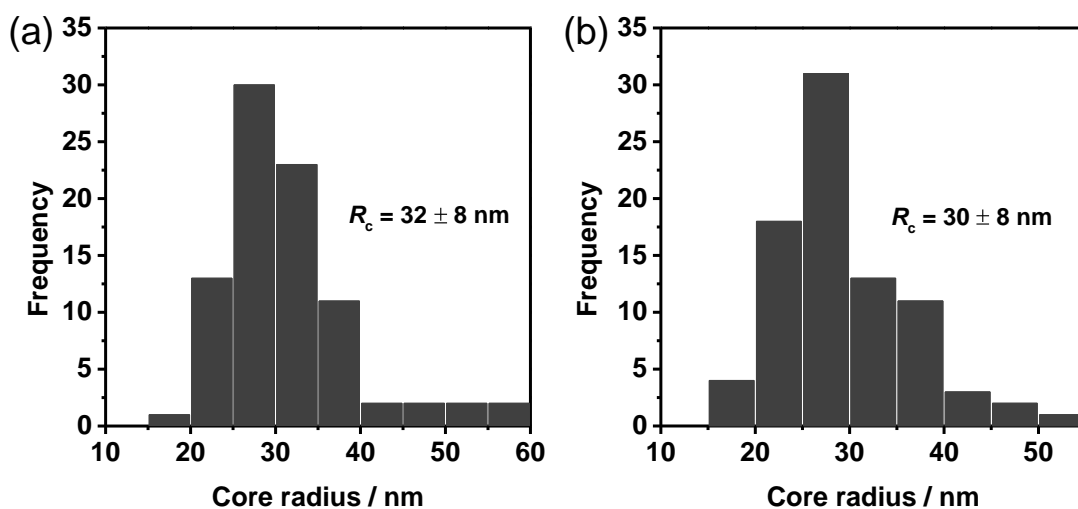


Figure S3. Histogram of core radius obtained from cryo-TEM images and the resulting mean and standard deviation of core radius for PEO DC (CR=1) (a) and PEO DC (CR=2) (b) aqueous dispersions.

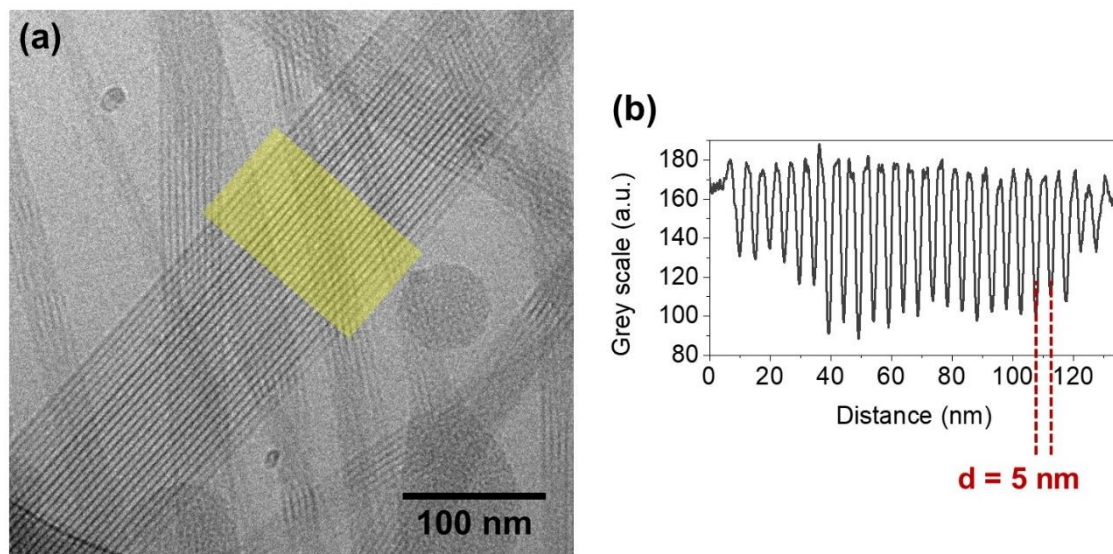


Figure S4. (a) Cryo-TEM image of the complex PEODC (CR=1) dispersed in water at 0.1 wt% of copolymer. (b) Intensity profile analysis of (a), from which a mean distance of 5.0 nm between the high contrast stripes was determined. This distance is interpreted as the inter-plane distance within the structure, see ref. G. Du, D. Belić, A. Del Giudice, V. Alfredsson, A. M. Carnerup, K. Zhu, B. Nyström, Y. Wang, L. Galantini and K. Schillén, *Angew. Chem. Int. Ed.*, 2022, **134**, 1–8.

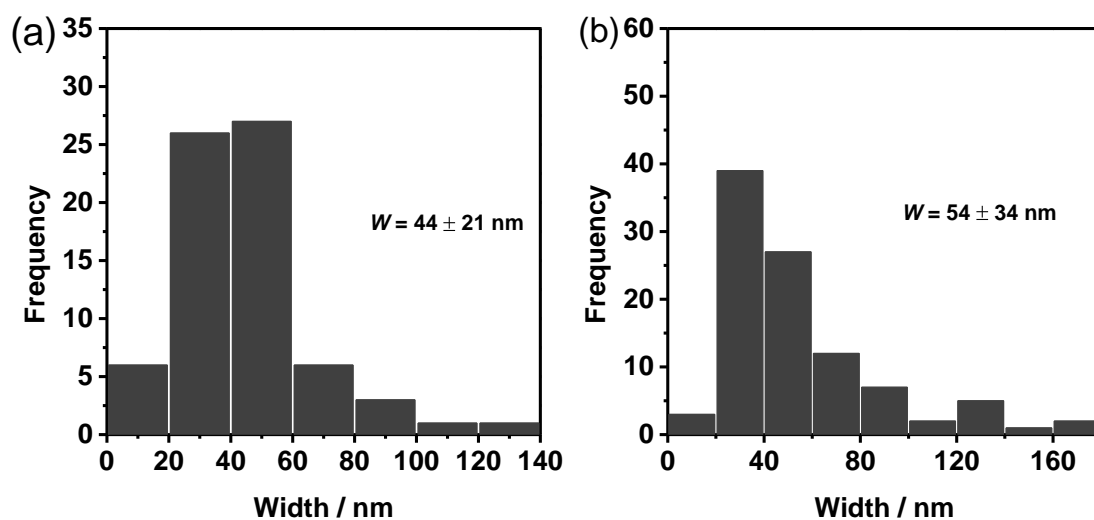


Figure S5. Histogram of ribbon width obtained from Cryo-TEM images and the resulting mean and standard deviation of ribbon width for PEODC (CR=1) (a) and PEODC (CR=2) (b) aqueous dispersions.

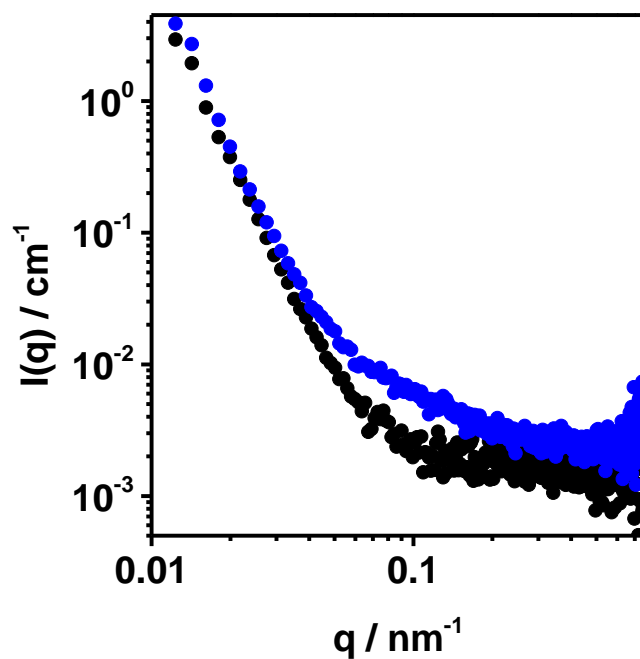


Figure S6. SAXS patterns of the complexes PEODC at CR = 1 (black curve) and CR = 2 (blue curve) dispersed in water with a copolymer concentration of 0.5 wt%.

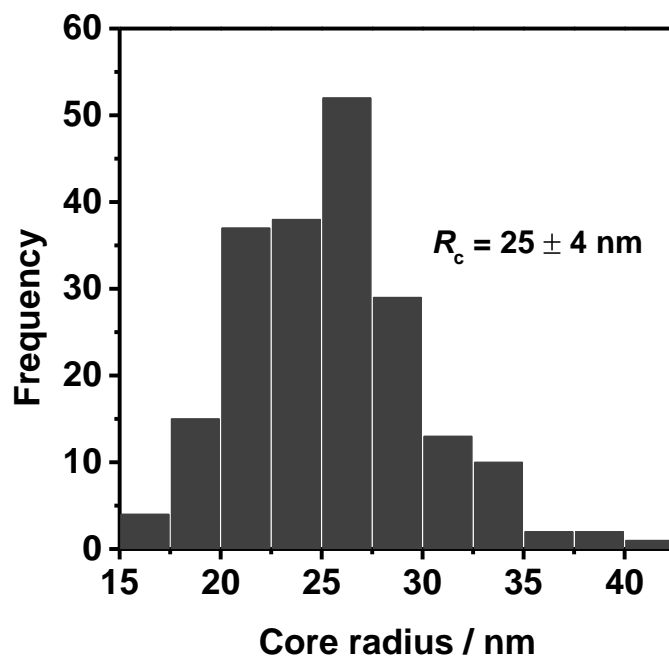


Figure S7. Histogram of core radius obtained by cryo-TEM images and the resulting mean and standard deviation of core radius for the collected top phase from a PEODC (CR=1) centrifuged dispersion.

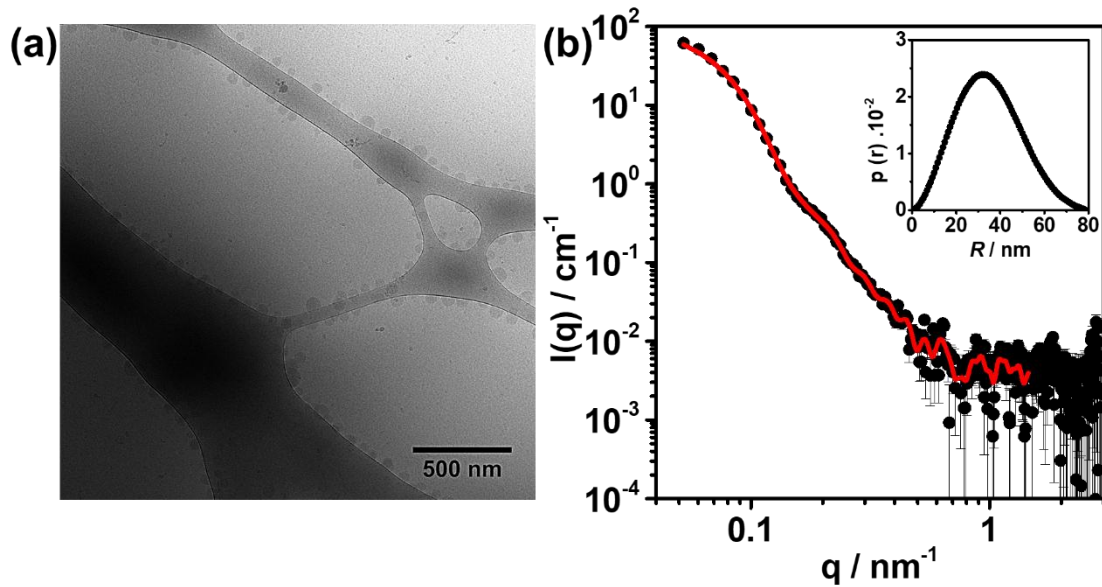


Figure S8. (a) Cryo-TEM image of the PEODC (CR=1) dispersion diluted to 0.1 wt% of copolymer and filtered through a 0.45 μm syringe filter. (b) Experimental SAXS profile (black symbols) and the curve fitting (red line) obtained from IFT analysis of the PEODC (CR=1) dispersion at 0.5 wt% of copolymer filtered through a 0.45 μm syringe filter. The inset corresponds to the $(p(r))$ curve obtained from IFT analysis.

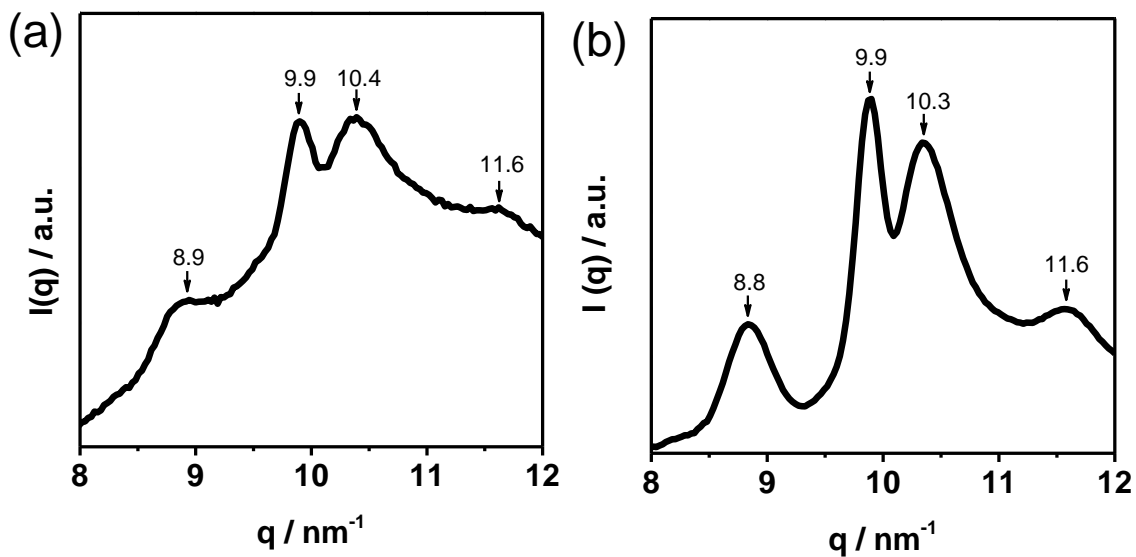


Figure S9. (a) WAXS curves of the bottom phase of the PEODC (CR=1) dispersion centrifuged and the (b) PEODC complex salt dispersion concentrated by centrifugation.

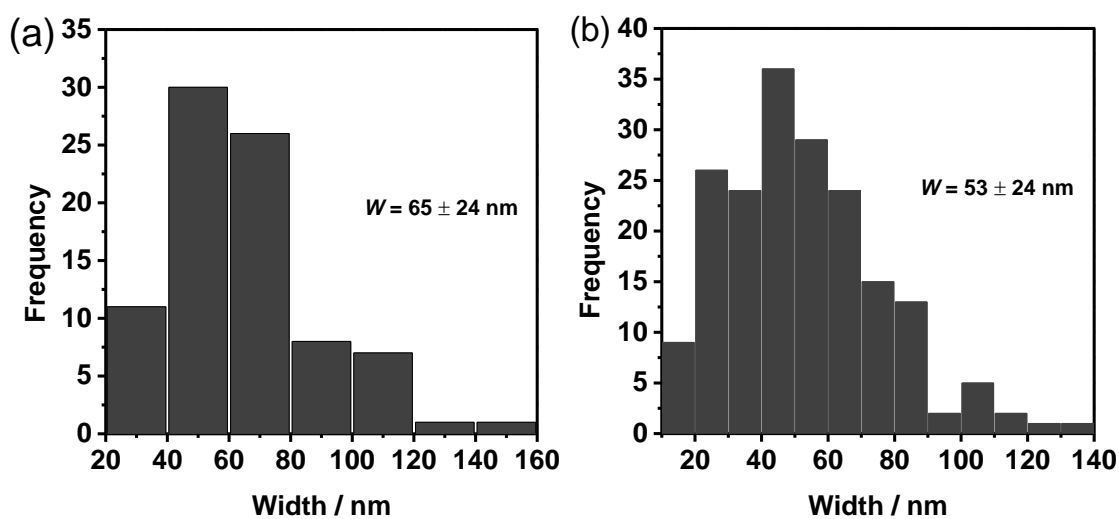


Figure S10. Histograms of ribbon width obtained from cryo-TEM images and the resulting mean and standard deviation of ribbon width for PEODC (CS) aqueous dispersions without (a) and with the addition of NaI (b) at an equivalent amount to that in the PEODC (CR=1) complex prepared by the direct mixing protocol.

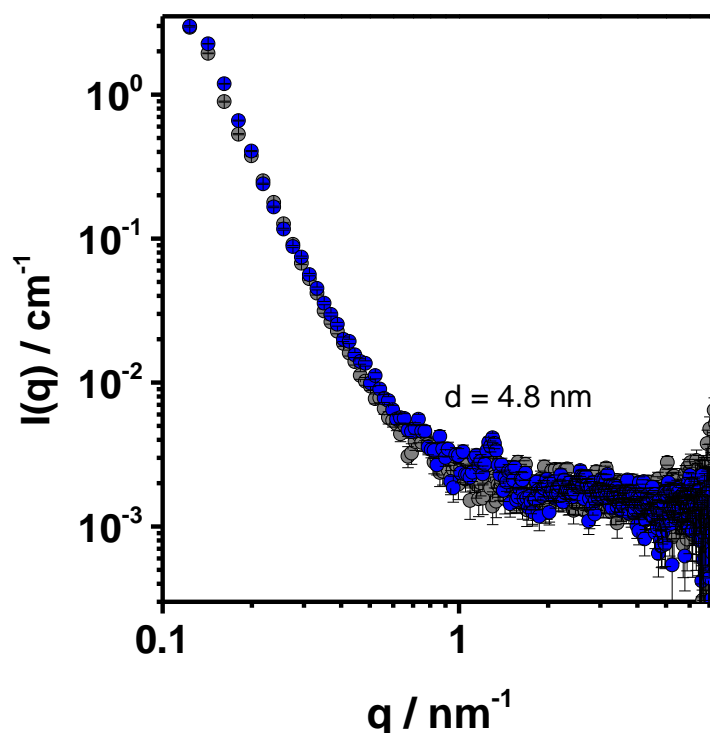


Figure S11. SAXS curves for a PEODC (CR=1) dispersion prepared by the direct mixing protocol (gray symbols; same as the black curve presented in Figure S6) and the same sample after freeze-drying and redispersion in water (blue symbols). The copolymer concentration was 0.5 wt%.

Table S1. Relative integrals of ^1H NMR peaks of the $\text{PEO}_{114}\text{-}b\text{-PTMAEMA}_{95}$ block copolymer solution and PEODC complexes. The integrals for N-methyl PTMAEMA(+) and DC peaks are presented relative to the PEO peak integral, which is used as an internal reference.

Samples	Relative integrals		
	PEO	N-methyl PTMAEMA(+)	DC
Block copolymer 0.5 wt %	1	1.88	-
PEODC (CR=1)	1	1.35	3.77
PEODC (CR=1) top phase	1	1.26	3.96
PEODC (CS)	1	1.05	2.66

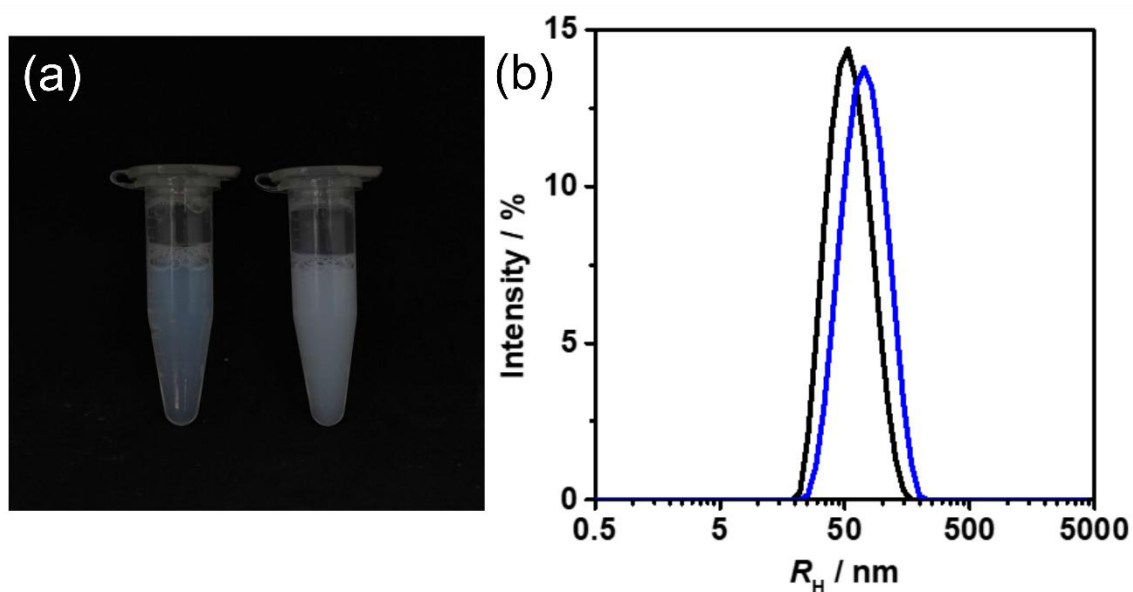


Figure S12. (a) Macroscopic images of PEODC (CR=1) dispersions prepared from stock solutions of different concentrations: 1 wt% of $\text{PEO}_{114}\text{-}b\text{-PTMAEMA}(+)_{95}$ and 2 wt% of NaDC (sample I); 2 wt% of $\text{PEO}_{114}\text{-}b\text{-PTMAEMA}(+)_{95}$ and 4 wt% of NaDC (sample II). Sample II has been diluted after mixing so that both samples have the same final composition with a copolymer concentration of 0.5 wt%. (b) The apparent hydrodynamic radii distribution obtained by DLS at 173° of the samples in (a) after further dilution to 0.05 wt% of copolymer, and filtering with a $0.45\ \mu\text{m}$ pore size filter. The temperature was 25°C .

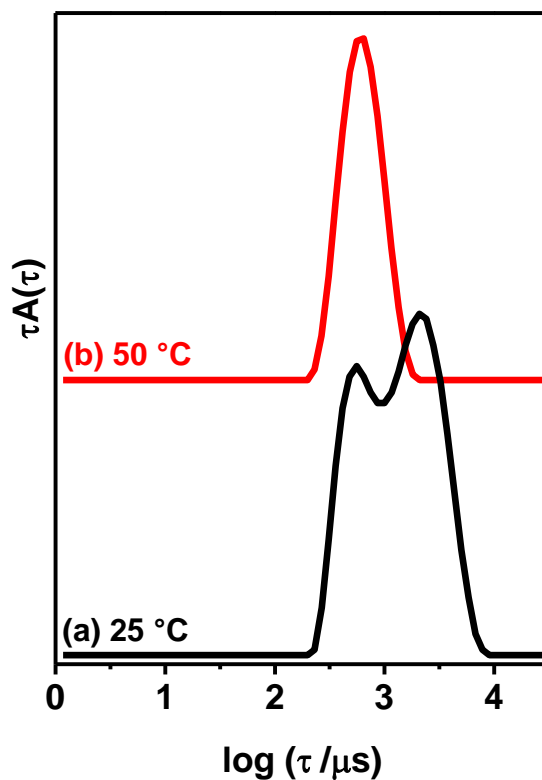


Figure S13. Relaxation time distributions obtained by non-linear least square fit of the intensity autocorrelation functions for PEO/DC (CS) dispersion measured at 25 °C (a) and 50 °C (b). The relaxation time distribution changes from multimodal (behavior in line with ref. K. Schillén, L. Galantini, G. Du, A. Del Giudice, V. Alfredsson, A. M. Carnerup, N. V. Pavel, G. Masci and B. Nyström, *Phys. Chem. Chem. Phys.*, 2019, **21**, 12518–12529) to monomodal after heating, consistent with the morphological transition observed by SAXS. The relaxation mode at 50 °C corresponds to a $R_{H,app} = 107$ nm. The x-axis is corrected for the change in absolute temperature and solvent viscosity relative to 25 °C by multiplying a correction factor of $(T/\eta_0)/(298/\eta_{298})$.

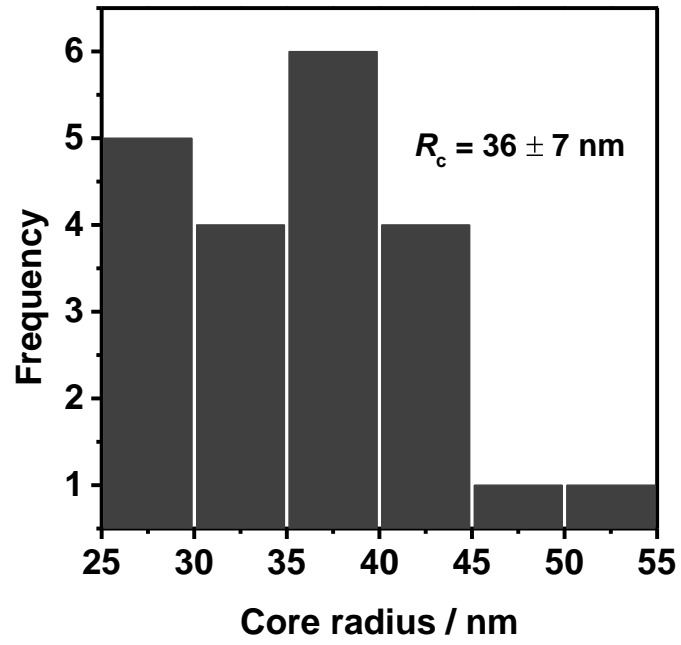


Figure S14. Histogram of core radius obtained by cryo-TEM images and the resulting mean and standard deviation of core radius for a PEOC (CR=1) aqueous dispersion.